HHS Public Access

Author manuscript

Nature. Author manuscript; available in PMC 2012 February 04.

Published in final edited form as:

Nature. ; 476(7358): 92–95. doi:10.1038/nature10206.

Photoentrainment and pupillary light reflex are mediated by distinct populations of ipRGCs

S.-K. Chen[1], **T.C. Badea**[2,*], and **S. Hattar**[1,3,*]

[1]Department of Biology, Johns Hopkins University, Baltimore, MD 21218, USA

[2]Retinal Circuit Development & Genetics Unit, N-NRL/NEI/NIH, Bethesda, MD 20892, USA

[3]Department of Neuroscience, Johns Hopkins University-School of Medicine, Baltimore, MD 21218, USA

Abstract

Intrinsically photosensitive retinal ganglion cells (ipRGCs) express the photopigment melanopsin and regulate a wide array of light-dependent physiological processes[1–11]. Genetic ablation of ipRGCs eliminates circadian photoentrainment and severely disrupts the pupillary light reflex (PLR)[12,13]. Here we show that ipRGCs consist of distinct subpopulations that differentially express the Brn3b transcription factor, and can be functionally distinguished. Brn3b-negative M1 ipRGCs innervate the suprachiasmatic nucleus (SCN) of the hypothalamus, whereas Brn3b-positive ipRGCs innervate all other known brain targets, including the olivary pretectal nucleus. Consistent with these innervation patterns, selective ablation of Brn3b-positive ipRGCs severely disrupts the PLR, but does not impair circadian photoentrainment. Thus, we find that molecularly distinct subpopulations of M1 ipRGCs, which are morphologically and electrophysiologically similar, innervate different brain regions to execute specific light-induced functions.

Keywords

Circadian photoentrainment; pupillary light reflex; outer retinal photoreceptors; ipRGCs; retinal ganglion cells; Brn3b; development and non-image forming visual functions

In addition to rod and cone photoreceptors, the retina contains a small subset of ipRGCs that express the photopigment melanopsin[1,9]. ipRGCs project to the suprachiasmatic nucleus (SCN) and the olivary pretectal nucleus (OPN), regions in the brain that control circadian rhythms and the pupillary light reflex (PLR), respectively. In the absence of the melanopsin protein (Opn4), ipRGCs lose their intrinsic photosensitivity[7], but still innervate the correct

*Correspondence and requests for materials should be addressed to S.H. (shattar@jhu.edu) or T.C.B. (tudor.badea@nih.gov). Editorial correspondence: Dr. Samer Hattar, Assistant Professor, Johns Hopkins University, Department of Biology, 3400 N. Charles Street/Mudd 227, Baltimore, MD 21218, Tel: 410-516-4231, fax: 410-516-5213, shattar@jhu.edu

Supplementary Information is linked to the online version of the paper at www.nature.com/nature.

Author Contributions S.K.C., T.C.B. and S.H. performed all experiments and wrote the paper.

Author Information Reprints and permissions information is available at http://www.nature.com/reprints/index.html.

The authors declare no competing financial interests.

brain regions[7] and convey rod/cone input[7,14,15] to drive non-image forming visual functions[7,16]. Recent studies have shown that ipRGCs are not uniform and can be further subdivided into distinct subtypes based on their morphology, electrophysiology and discrete brain targets[2,17]. M1 ipRGCs can be readily distinguished from other ipRGC subtypes (herein referred to as non-M1 ipRGCs) because they are the only subtype with exclusive dendritic stratification in the OFF sublamina of the inner plexiform layer (IPL) in the retina[18,19]. The prevailing view is that M1 ipRGCs are a homogeneous population that send collateral axonal branches to two relay nuclei, the SCN and OPN, to drive circadian photoentrainment and PLR[20]. Genetic ablation of ipRGCs by diphtheria toxin (in Opn4^{aDTA} mice) eliminates circadian photoentrainment and disrupts PLR[12]. Here we surprisingly found that M1 ipRGCs are not a uniform population, but consist of functionally distinct subpopulations defined by their expression of the POU domain transcription factor, Brn3b.

Previously, we showed that *brn3b* mutant mice, which lack 80% of RGCs, have pronounced deficits in PLR, but are still capable of weak photoentrainment[21]. These findings raise the possibility that the remaining Brn3b-negative M1 ipRGCs selectively mediate photoentrainment. To determine the extent of Brn3b expression in the M1 ipRGC population, we performed anti-Brn3b immunohistochemistry on retinas from Opn4$^{tau\text{-}lacZ}$ mice, together with X-gal staining that labels only M1 ipRGCs[21]. A fraction of β-gal positive RGCs stained for Brn3b in the adult retina (Figure 1a).

To determine the projections of Brn3b-positive ipRGCs, we mated mice in which inducible Cre recombinase is driven by the melanopsin promoter (*Opn4*$^{CreERT2/+}$) to mice having either a ubiquitous Cre-dependent Alkaline Phosphatase (AP) reporter (*Rosa26-IAP*)[22] or a conditional Brn3b knock-in (*Brn3b*$^{CKOAP/+}$)[21] in which Cre recombination causes the AP coding region to be expressed by the Brn3b promoter (Supplementary Figure 1). Tamoxifen injections in *Opn4*$^{CreERT2/+}$*; R26*$^{IAP/+}$ animals results in labeling of M1 and non-M1 ipRGCs by AP histochemistry (Figure 1c), but only Brn3b-expressing ipRGCs in *Opn4*$^{CreERT2/+}$*; Brn3b*$^{CKOAP/+}$ animals (Figure 1b and Supplementary Table 1). AP labeling of Brn3-positive ipRGCs allowed us to analyze the dendritic arbors and central projections of these cells, independent of Brn3b-negative ipRGCs (Figure 1b, d–f). Many Brn3b-positive ipRGCs had dendrites arborizing in the ON sublamina of the IPL similar to previous observations for non-M1 ipRGCs[2,18,20,23]. This indicates that Brn3b expression is not just restricted to M1 ipRGCs, but is also expressed in non-M1 ipRGCs (Figure 1b). Comparing the labeling of Brn3b-positive M1 and non-M1 ipRGCs with all ipRGC subtypes, we find that most brain targets of ipRGCs show similar patterns of innervation (Figure 1d–i). In particular, the OPN is innervated fully in both cases (Figure 1f and 1i). However, a notable difference is found in the SCN; in the *Opn4*$^{CreERT2/+}$*; R26*$^{IAP/+}$ mice, the SCN was completely innervated by AP positive ipRGC fibers (Figure 1g) similar to previous studies[2]. In contrast, in the *Opn4*$^{CreERT2/+}$*; Brn3b*$^{CKOAP/+}$ mice, the SCN was sparsely innervated by Brn3b-positive ipRGCs (Figure 1d), with the medial regions of the SCN completely devoid of innervation (Figure 1d). We further confirmed that the diminished SCN innervation is not due to the use of the inducible Opn4^{CreERT2} line, since crossing the Opn4^{Cre} line[2], with the Brn3b-knock-in allele (*Opn4*^{Cre}*; Brn3b*$^{CKOAP/+}$

animals), also results in reduced SCN innervation (Supplementary Figure 2). Thus, ipRGCs can be separated into two subpopulations based on their Brn3b expression and connectivity.

To label the central projection of Brn3b-negative ipRGCs and determine the physiological functions of both Brn3b-negative and Brn3b-positive ipRGCs, we specifically eliminated cells that co-express melanopsin and Brn3b by crossing $Opn4^{Cre}$ and $Brn3b^{Z\text{-}dta}$ lines (Supplementary Table 1). The $Brn3b^{Z\text{-}dta}$ knock-in line[24] expresses diphtheria toxin A subunit (DTA) from the endogenous *Brn3b* gene promoter (Supplementary Figure 1) only in the presence of Cre[25]. Thus, in $Opn4^{Cre/+}$; $Brn3b^{Z\text{-}dta/+}$ mice, Brn3b-expressing ipRGCs are ablated, whereas Brn3b negative ipRGCs and conventional (melanopsin negative) RGCs are left intact (Supplementary Figure 3). Using melanopsin immunofluorescence that only reveals M1 ipRGCs in $Opn4^{Cre/+}$; $Brn3b^{Z\text{-}dta/+}$ retinas, we observed less than 200 surviving M1 ipRGCs (Figure 2a, and b). To determine the extent of ablation of all ipRGCs in the $Opn4^{Cre/+}$; $Brn3b^{Z\text{-}dta/+}$ mice, we generated triple heterozygous $Opn4^{Cre/+}$; $Brn3b^{Z\text{-}dta/+}$; *Z/AP* (Supplementary Table 1) mice, in which AP labeling in the presence of Cre ($Opn4^{Cre/+}$; *Z/AP*) reveals all M1 and non-M1 ipRGCs (~2000 cells)[2]. Using AP histochemistry in $Opn4^{Cre/+}$; $Brn3b^{Z\text{-}dta/+}$; *Z/AP* mice, we observed similar numbers of surviving ipRGCs as with melanopsin immunofluorescence (Figure 2a). These results show that all non-M1 cells are ablated and that the surviving 10% (200 out of 2000) of total ipRGCs are Brn3b-negative and belong to the M1 subtype.

To assess the central projections of these surviving M1 Brn3b-negative ipRGCs, we crossed $Opn4^{Cre/+}$; $Brn3b^{Z\text{-}dta/+}$ mice with the either the $Opn4^{tau\text{-}LacZ}$ reporter[19,20] or Z/AP reporter[26]. Although only 200 M1 ipRGCs remained in the $Opn4^{Cre/tau\text{-}LacZ}$; $Brn3b^{Z\text{-}dta/+}$ or $Opn4^{Cre/+}$; $Brn3b^{Z\text{-}dta/+}$; *Z/AP* mice, we observed that their fibers completely innervated the SCN at levels comparable to those observed in the control groups (Figure 2c). However, innervation of the intergeniculate nucleus (IGL) was highly attenuated (Figure 2d) and OPN projections were completely abolished (Figure 2e). Interestingly, the shell of the OPN showed no fibers in the $Opn4^{Cre/tau\text{-}LacZ}$; $Brn3b^{Z\text{-}dta/+}$ as compared to control mice (Figure 2e). Given that both the SCN and OPN shell are innervated by M1 ipRGCs[5,20], differential labeling of these ipRGC targets in $Opn4^{Cre/tau\text{-}LacZ}$; $Brn3b^{Z\text{-}dta/+}$ mice shows that the M1 subtype of ipRGCs is not a uniform population. To ensure that RGCs that are not intrinsically photosensitive are intact in the $Opn4^{Cre/+}$; $Brn3b^{Z\text{-}dta/+}$ mice, we used cholera toxin injection in the eye to label all RGC fibers in the brain anterogradely. RGCs innervated the dorsal and ventral lateral geniculate nuclei (dLGN and vLGN) normally in these mice (figure 2f). This is further supported by the similar visual acuity measured in $Opn4^{Cre/+}$; $Brn3b^{Z\text{-}dta/+}$ and wild type mice (Figure 2g).

Given that ipRGC projections to the OPN are lost, but SCN projections are largely intact, the $Opn4^{Cre/+}$; $Brn3b^{Z\text{-}dta/+}$ mice allow the relative contributions of Brn3b-negative ipRGCs to the pupillary light reflex (PLR) and circadian light responses to be determined. We first measured PLR in $Opn4^{Cre/+}$; $Brn3b^{Z\text{-}dta/+}$ mice at two light intensities in the middle of the day (ZT 8). The pupil of wild type mice is 95.61% constricted under high light intensity and 79.47% under low light intensity (Figure 3a and c). In contrast, $Opn4^{Cre/+}$; $Brn3b^{Z\text{-}dta/+}$ mice showed a highly attenuated PLR at ZT 8 under high and low light intensities (Figure 3b and c). This phenotype is remarkably similar to the PLR deficits observed in

Opn4$^{aDTA/aDTA}$ homozygous animals[12]. We further investigated the PLR in the middle of the night (ZT20), and found that *Opn4*$^{Cre/+}$*; Brn3b*$^{Z\text{-}dta/+}$ animals have no pupillary constriction to high or low light stimulations (Supplementary Figure 4 and Supplementary Text). The residual PLR response at ZT 8 in *Opn4*$^{aDTA/aDTA}$ and *Opn4*$^{Cre/+}$*; Brn3b*$^{Z\text{-}dta/+}$ mice suggests that other melanopsin negative RGCs contribute to this reflex. One candidate population could be Brn3a positive RGCs, which project to the OPN[21].

We then asked whether the surviving M1 ipRGCs that innervate the SCN in *Opn4*$^{Cre/+}$*; Brn3b*$^{Z\text{-}dta/+}$ mice are sufficient to drive circadian photoentrainment. Strikingly, we found that *Opn4*$^{Cre/+}$*; Brn3b*$^{Z\text{-}dta/+}$ mice are able to photoentrain as well as controls under normal 24-hr light dark cycles or skeleton photoperiods (Figure 4a and c, Supplementary Figures 5 and 6, and Supplementary Text). In addition, they can readjust to a “jet-lag” light-dark cycle paradigm with advanced and delayed dark onsets (Figure 4a). We also observed no difference in activity during the dark phase of the ultradian[16] 3.5:3.5 LD cycle (Figure 4b and d). Moreover, a 15 min light pulse presented early during the active phase of mice maintained under constant conditions generated similar phase shifts (76.2±6.5 and 70.67±7.3 minutes for control and Opn4$^{cre/+}$; Brn3b$^{Z\text{-}dta/+}$ animals, respectively; Figure 4e). Together, these results indicate that Brn3b-negative ipRGCs, comprising only 10% of all identified ipRGC subtypes, are sufficient for circadian photoentrainment. However, *Opn4*$^{cre/+}$*; Brn3b*$^{Z\text{-}dta/+}$ mice exhibit a minor deficit in period lengthening under constant light conditions (Figure 4f). Since period lengthening is positively correlated with light intensity, attenuated projections to the IGL in *Opn4*$^{Cre/+}$*; Brn3b*$^{Z\text{-}dta/+}$ mice could underlie this difference.

Here we show that, although M1 ipRGCs have homogeneous morphological and electrophysiological characteristics, they consist of at least two different subpopulations, which can be discriminated by expression of the Brn3b transcription factor (Figure 4g). The two M1 subpopulations have distinct brain targets and are involved in different non-image forming visual functions. Using precise molecular genetic tools to ablate Brn3b-expressing ipRGCs, we disrupted the pupillary light reflex but not circadian photoentrainment. Thus, ipRGCs have parallel pathways for controlling non-image forming functions, analogous to the specialized properties of RGCs that mediate image-forming functions[27].

Methods Summary

Animals

All experiments were conducted in accordance with NIH guidelines and approved institutional animal care and use committees of the Johns Hopkins University.

Behavioral analyses

We used previously described behavioral tests[12] that measure visual acuity (optomotor), pupil constriction (PLR), the period of the circadian oscillator (wheel running activity), the adjustment of the circadian clock to different light stimulations (circadian photoentrainment, “jet-lag” paradigms, phase shifting, and skeleton photoperiod) and direct light effects on activity (constant light and ultradian).

Histology

X-gal and AP histochemistry were performed as described previously[2,5,28].

Methods

Mice

All mice were of a mixed background (BL/6;129SvJ). Littermates male animals that were used in the behavioral analyses aged between 4 and 12 months. Animals were housed and treated in accordance with NIH and IACUC guidelines, and used protocols approved by the Johns Hopkins University Animal Care and Use Committees.

Generation of Opn4^{CreERT2} line

To generate Opn4-CreERT2 mice, we used the targeting arms and general strategy detailed in reference number 2. The only difference is that the construct contained a rabbit β-globin intron, CreERT2 recombinase and an IRESLacZ cassette immediately downstream of the start codon for mouse melanopsin.

Immunohistochemistry

Mouse retina was fixed as whole eyecup for at least 30 min in 4% PFA and cryoprotected in 30% sucrose overnight. 40 μm retina sections were obtained by cryostat and incubated with blocking solution (0.3% Triton X-100 and 5% normal goat serum in PBS) for 1 hour before staining with primary antibody overnight at 4°C. Sections were washed in 1X PBS 3 times for 30 minutes and incubate with secondary antibody at room temperature for 2 hours before mounting in vector-shield mounting solution. Images were taken with Olympus microscope with epi-fluorescence. The dilution for melanopsin antibody (Advanced Targeting Systems) is 1:1000.

Tamoxifen injections

The intensity of labeling depends on the amount of tamoxifen injected into animals as well as the efficiency of excision from loxP regions in the reporter mice. Therefore, all intraperitoneal (IP) injections of tamoxifen were standardized to label all the identified ipRGC subtypes (M1–M5). In fact, ipRGCs with morphologies characteristic for all identified ipRGC subtypes are observed in the flat mount retinas in Figure 2b and c. Retina shown in Figure 2b was from an animal injected with 500 μg of tamoxifen at P14. Brains shown in Figure 2d–f, were from an animal injected with 250 μg of tamoxifen at P5. For Figure 2c and g-I, images are from an animal injected with 1 mg tamoxifen at E17. There is no significance to injecting tamoxifen at different postnatal times. We simply use the AP staining as a tracing method to reveal ipRGC targets in the brain.

Histology

X-gal staining—Mice were perfused with 15 ml of 4% PFA, the brain was dissected out, cryoprotected in 30% sucrose for 2 days and 50 μm coronal sections were obtained by cryostat. Brain sections were incubated in staining solution with 1mg/ml X-gal for 2 days at room temperature, post fixed in 4% PFA for an hour and mounted with glycerol.

Alkaline phosphatase (AP) staining—Mice were perfused with 45 ml of 4% PFA, the brain and retina were dissected out. Whole mount retina was post fixed for 30 min and 200 μm coronal brain sections were obtained by vibrotome. Both retina and brain sections were heat inactivated in 65°C for 90 minutes and incubated in AP staining solution. After staining, the sections and retina whole mount were post fixed in 4% PFA for overnight and washed with ethanol series before mounting.

Cholera toxin injections in the eye

Mice were anaesthetized with Avertin. Eyes were injected intravitreally with 2 μl of cholera toxin B subunit conjugated with Alexa Fluor 488 or Alexa Fluor 555 (Invitrogen). Three days after injection, brains were isolated, sectioned and mounted.

Visual acuity

A virtual cylinder OptoMotry (Cerebral Mechanics) was used to determine visual acuity by measuring the image-tracking reflex of mice. A sine-wave grating was projected on the screen rotating in a virtual cylinder. The animal was assessed for a tracking response on stimulation for about 5s. All acuity thresholds were determined by using the staircase method with 100% contrast.

Pupillary Light Reflex

All animals were kept under 12:12 LD cycle before testing PLR. Before each experiment, all animals were dark-adapted for at least 1h. While one eye received light stimulation with specific intensity described in the main text from a 470-nm light-emitting-diode light source (Super Bright LEDs), a digital camcorder (DCRHC96; Sony) was used to record from the other eye (for 30s) at 30 frames.s^{-1} under a 940-nm light (LDP). The percentage pupil constriction was calculated as the percentage of pupil area at 30s after initiation of the stimulus (steady state) relative to the dilated pupil size (right before light stimulation). Same group of animals were used for wheel running activity. The control animals are littermates to the experimental animals ($Opn4^{Cre/+}$; $Brn3b^{Z\text{-}dta/+}$) with either $Opn4^{Cre/+}$; $Brn3b^{+/+}$ or $Opn4^{+/+}$; $Brn3b^{Z\text{-}dta/+}$ genotypes.

Wheel running activity

Mice were placed in cages with a 4.5-inch running wheel, and their activity was monitored with VitalView software (MiniMitter). The period was calculated with ClockLab (Actimetrics). Mice were initially placed under 12:12 light dark cycle for 2 weeks. Animals were then exposed to two “jet-lag” light paradigms: 10 days of a 6-h advance followed by 10 days of a 6-h delay. After the “jet-lag” paradigms, mice were kept under constant darkness for 2 weeks followed by 10 days of constant light. Phase-shifting experiments were carried out on the 7th day of constant darkness where each animal was exposed to a 15 min light pulse at CT16 (1,500lx). Animals were re-entrained to 12:12 LD cycle for 2 weeks before exposing them to ultradian 3.5:3.5 light/dark cycles. The intensity of light for all the light dark cycle were ~1,000lx. Another set of mice was tested using a skeleton photoperiod, where two 1-hr light pulses (800lx) separated by 10 hours of dark were administered.

Supplementary Material

Refer to Web version on PubMed Central for supplementary material.

Acknowledgments

We thank the extreme generosity of Dr. Jeremy Nathans for providing several animal lines (Brn3b^{CKOAP}, R26^{IAP} and Z/AP) that were crucial for the completion of this study. We thank Dr. Jennifer L. Ecker who created the inducible cre line (Opn4^{CreERT2}) we used in this study. We thank Dr. Zhiyong Yang in Dr. Don Zack's laboratory for providing the Brn3b$^{Z\text{-}dta}$ mouse line, which was generously provided by the original laboratory that created this line: Dr. William Klein. We also thank Dr. Rejji Kuruvilla, Dr. Haiqing Zhao, Dr. Marnie Halpern, Dr. A.P. Sampath and Dr. Tiffany Schmidt for their careful reading of the manuscript and helpful suggestions and the Johns Hopkins University Mouse Tri-Lab for support. This work was supported by the National Institutes of Health grant GM076430 (S.H.), the David and Lucile Packard Foundation (S.H.), and the Alfred P. Sloan Foundation (S.H.).

References

1. Berson DM, Dunn FA, Takao M. Phototransduction by retinal ganglion cells that set the circadian clock. Science. 2002; 295 (5557):1070–1073. [PubMed: 11834835]
2. Ecker JL, et al. Melanopsin-expressing retinal ganglion-cell photoreceptors: cellular diversity and role in pattern vision. Neuron. 2010; 67 (1):49–60. [PubMed: 20624591]
3. Gooley JJ, Lu J, Fischer D, Saper CB. A broad role for melanopsin in nonvisual photoreception. J Neurosci. 2003; 23 (18):7093–7106. [PubMed: 12904470]
4. Hannibal J, Fahrenkrug J. Melanopsin containing retinal ganglion cells are light responsive from birth. Neuroreport. 2004; 15 (15):2317–2320. [PubMed: 15640747]
5. Hattar S, Liao HW, Takao M, Berson DM, Yau KW. Melanopsin-containing retinal ganglion cells: architecture, projections, and intrinsic photosensitivity. Science. 2002; 295 (5557):1065–1070. [PubMed: 11834834]
6. Hattar S, et al. Melanopsin and rod-cone photoreceptive systems account for all major accessory visual functions in mice. Nature. 2003; 424 (6944):76–81. [PubMed: 12808468]
7. Lucas RJ, et al. Diminished pupillary light reflex at high irradiances in melanopsin-knockout mice. Science. 2003; 299 (5604):245–247. [PubMed: 12522249]
8. Panda S, et al. Melanopsin (Opn4) requirement for normal light-induced circadian phase shifting. Science. 2002; 298 (5601):2213–2216. [PubMed: 12481141]
9. Provencio I, Rollag MD, Castrucci AM. Photoreceptive net in the mammalian retina. Nature. 2002; 415 (6871):493. [PubMed: 11823848]
10. Ruby NF, et al. Role of melanopsin in circadian responses to light. Science. 2002; 298 (5601): 2211–2213. [PubMed: 12481140]
11. Tu DC, et al. Physiologic diversity and development of intrinsically photosensitive retinal ganglion cells. Neuron. 2005; 48 (6):987–999. [PubMed: 16364902]
12. Guler AD, et al. Melanopsin cells are the principal conduits for rod-cone input to non-image-forming vision. Nature. 2008; 453 (7191):102–105. [PubMed: 18432195]
13. Hatori M, et al. Inducible ablation of melanopsin-expressing retinal ganglion cells reveals their central role in non-image forming visual responses. PLoS ONE. 2008; 3 (6):e2451. [PubMed: 18545654]
14. Schmidt TM, Taniguchi K, Kofuji P. Intrinsic and extrinsic light responses in melanopsin-expressing ganglion cells during mouse development. J Neurophysiol. 2008; 100 (1):371–384. [PubMed: 18480363]
15. Wong KY, Dunn FA, Graham DM, Berson DM. Synaptic influences on rat ganglion-cell photoreceptors. J Physiol. 2007; 582 (Pt 1):279–296. [PubMed: 17510182]
16. Mrosovsky N, Hattar S. Impaired masking responses to light in melanopsin-knockout mice. Chronobiol Int. 2003; 20 (6):989–999. [PubMed: 14680139]

17. Brown TM, et al. Melanopsin contributions to irradiance coding in the thalamo-cortical visual system. PLoS Biol. 2010; 8 (12):e1000558. [PubMed: 21151887]
18. Berson DM, Castrucci AM, Provencio I. Morphology and mosaics of melanopsin-expressing retinal ganglion cell types in mice. J Comp Neurol. 2010; 518 (13):2405–2422. [PubMed: 20503419]
19. Hattar S, et al. Central projections of melanopsin-expressing retinal ganglion cells in the mouse. J Comp Neurol. 2006; 497 (3):326–349. [PubMed: 16736474]
20. Baver SB, Pickard GE, Sollars PJ. Two types of melanopsin retinal ganglion cell differentially innervate the hypothalamic suprachiasmatic nucleus the olivary pretectal nucleus. Eur J Neurosci. 2008; 27 (7):1763–1770. [PubMed: 18371076]
21. Badea TC, Cahill H, Ecker J, Hattar S, Nathans J. Distinct roles of transcription factors brn3a and brn3b in controlling the development, morphology, and function of retinal ganglion cells. Neuron. 2009; 61 (6):852–864. [PubMed: 19323995]
22. Badea TC, et al. New mouse lines for the analysis of neuronal morphology using CreER(T)/loxP-directed sparse labeling. PLoS ONE. 2009; 4 (11):e7859. [PubMed: 19924248]
23. Schmidt TM, Kofuji P. Functional and morphological differences among intrinsically photosensitive retinal ganglion cells. J Neurosci. 2009; 29 (2):476–482. [PubMed: 19144848]
24. Mu X, et al. Ganglion cells are required for normal progenitor-cell proliferation but not cell-fate determination or patterning in the developing mouse retina. Curr Biol. 2005; 15 (6):525–530. [PubMed: 15797020]
25. Gan L, Wang SW, Huang Z, Klein WH. POU domain factor Brn-3b is essential for retinal ganglion cell differentiation and survival but not for initial cell fate specification. Dev Biol. 1999; 210 (2): 469–480. [PubMed: 10357904]
26. Lobe CG, et al. Z/AP, a double reporter for cre-mediated recombination. Dev Biol. 1999; 208 (2): 281–292. [PubMed: 10191045]
27. Wassle H. Parallel processing in the mammalian retina. Nat Rev Neurosci. 2004; 5 (10):747–757. [PubMed: 15378035]
28. Badea TC, Wang Y, Nathans J. A noninvasive genetic/pharmacologic strategy for visualizing cell morphology and clonal relationships in the mouse. J Neurosci. 2003; 23 (6):2314–2322. [PubMed: 12657690]

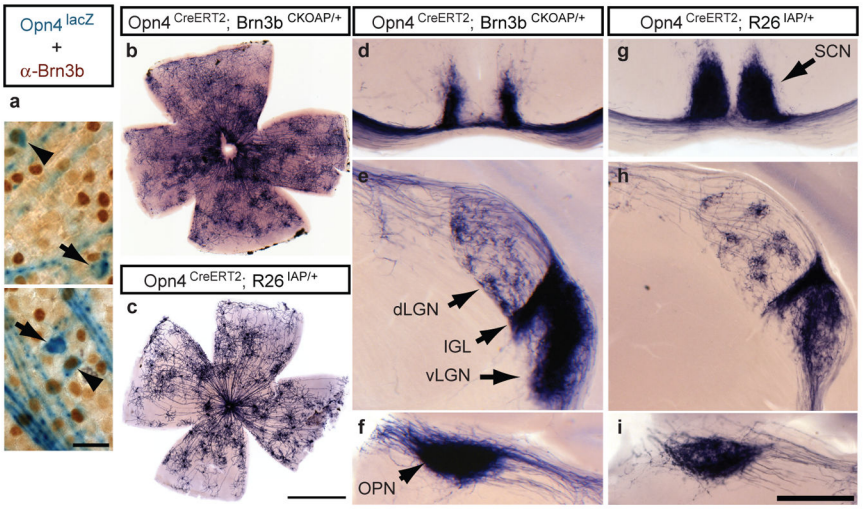

Figure 1. Co-expression of Melanopsin and Brn3b defines a specific set of ipRGCs

a, Retinal flat mounts from *Opn4*$^{tau\text{-}LacZ/+}$ mice stained with anti-Brn3b antibody (brown) and X-gal staining (blue) show Brn3b-positive (arrowheads; 140 Brn3b-positive ipRGCs from 988 lacZ+ cells, n=5) and Brn3b-negative (arrows), M1 ipRGCs. b–i, AP histochemistry of retina (b and c) and coronal brain sections (d–i) from *Opn4*$^{CreERT2/+}$;*Brn3b*$^{CKOAP/+}$ mice (b, d–f), or from *Opn4*$^{CreERT2/+}$;*R26*$^{IAP/+}$ mice (c, g–i). Suprachiasmatic region shows partial innervation in *Opn4*$^{CreERT2/+}$;*Brn3b*$^{CKOAP/+}$ mice (d), compared to full innervation of the SCN in *Opn4*$^{CreERT2/+}$;*R26*$^{IAP/+}$ mice (g). Both mouse lines show significant ipRGC projections to the IGL and vLGN, and sparse innervation to the dLGN (e and h) and intense labeling of the OPN (f and i). Scale bars are 25 μm (a), 1 mm (b and c), and 400 μm (d–i).

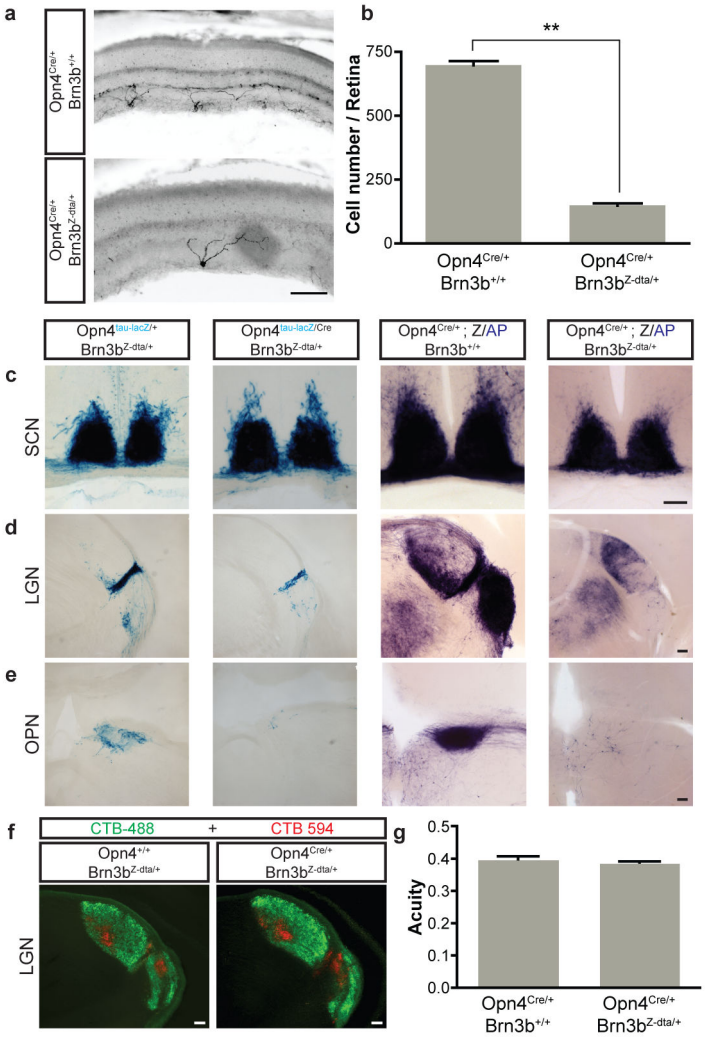

Figure 2. Genetic ablation of Brn3b-positive ipRGCs does not impair targeting to the SCN

a, Melanopsin immunofluorescence reveals a reduction in ipRGC numbers in *pn4*$^{Cre/+}$;*Brn3b*$^{Z\text{-}dta/+}$ retina compared to control (*Opn4*$^{Cre/+}$;*Brn3b*$^{+/+}$). b, Quantification of surviving melanopsin-positive cells in *Opn4*$^{Cre/+}$;*Brn3b*$^{Z\text{-}dta/+}$ (149.8±8.65 cells/retina; n=4) and control (698.8±16.85 cells/retina; n=4) mice. c–e, Coronal brain sections of *pn4*$^{tau\text{-}LacZ/+}$;*Brn3b*$^{Z\text{-}dta/+}$ and *Opn4*$^{Cre/tau\text{-}LacZ}$;*Brn3b*$^{Z\text{-}dta/+}$ (c–e, left two panels), and *pn4*$^{Cre/+}$;*Brn3b*$^{+/+}$;*Z/AP* and *Opn4*$^{Cre/+}$;*Brn3b*$^{Z\text{-}dta/+}$;*Z/AP* (c–e, right two panels) mice using X-gal (c–e, left two panels) or AP histochemistry (c–e, right two panels). Sections show SCN (c), LGN (d), and OPN (e). i, Labeling of all RGCs with Alexa Fluor 594- and 488-conjugated Cholera toxin B in the left eye (red) and the right eye (green), respectively shows normal brain targeting to image forming regions. j, Visual acuity was the same between *Opn4*$^{+/+}$;*Brn3b*$^{Z\text{-}dta/+}$ (n=5) and *Opn4*$^{Cre/+}$;*Brn3b*$^{Z\text{-}dta/+}$ mice (n=6). Scale bars are 100 μm. Error bars represent SEMs.

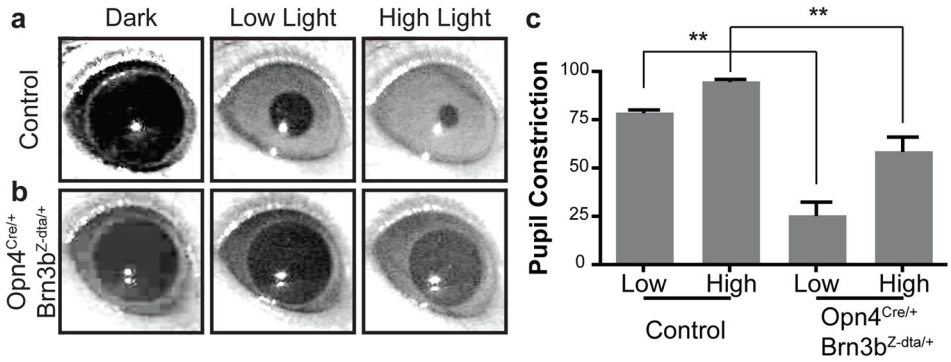

Figure 3. *Opn4*$^{Cre/+}$;*Brn3*$^{Z\text{-}dta/+}$ mice show severe deficits in the pupillary light reflex PLR)

a–b, Representative images of PLR from control and *Opn4*$^{Cre/+}$;*Brn3b*$^{Z\text{-}dta/+}$ mice. Left panels show pupils under dark conditions, middle panels show pupils under low light intensity (22 μW/cm^2) and right panels show pupils under high light intensity (5.66 mW/cm^2). c, Quantification of PLR data from control (n=5) and *Opn4*$^{Cre/+}$;*Brn3b*$^{Z\text{-}dta/+}$ n=6) animals. ** indicates $p<0.01$ with 1-way ANOVA. Error bars represent SEMs.

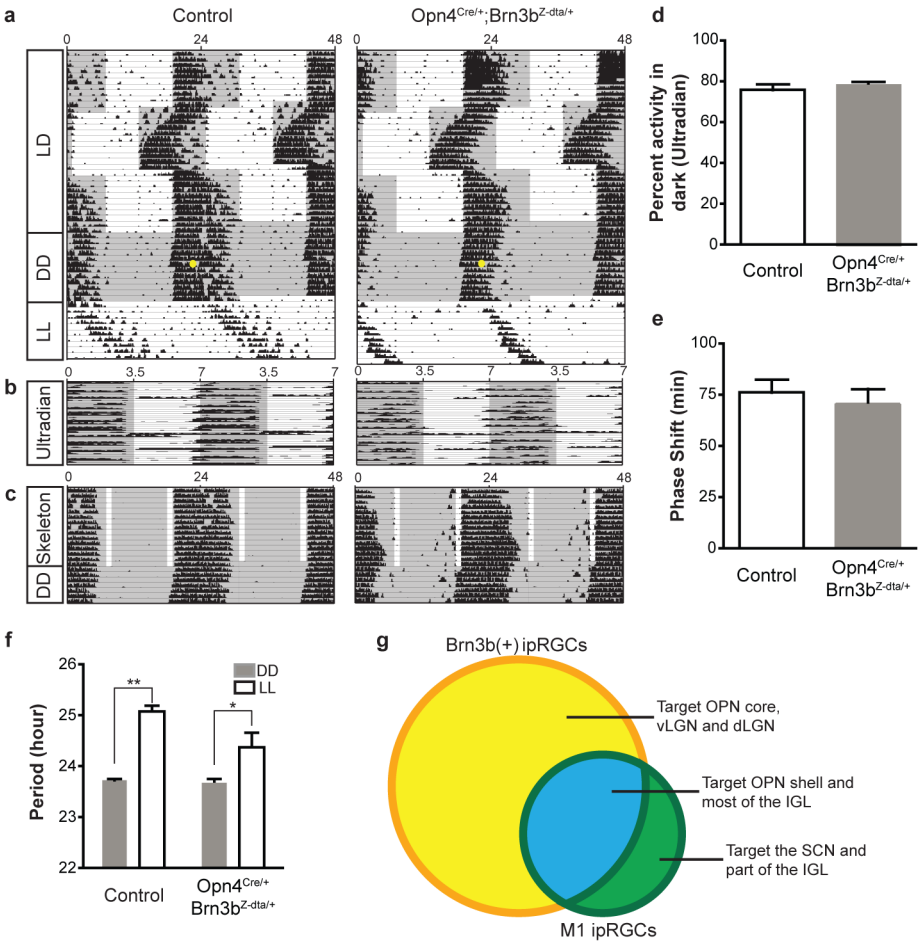

Figure 4. *Opn4*$^{Cre/+}$;*Brn3b*$^{Z\text{-}dta/+}$ mice show normal circadian photoentrainment

a–c, Representative actograms from control and *Opn4*$^{Cre/+}$;*Brn3b*$^{Z\text{-}dta/+}$ animals under a series of lighting paradigms: a, 12:12 hours LD cycle, “jet-lag”, constant darkness (DD), and constant light (LL); b, Ultradian 3.5:3.5 hours cycles; c, skeleton photoperiod. The gray background indicates darkness and the yellow dot indicates the 15 minutes light pulse at CT 16. *Opn4*$^{Cre/+}$;*Brn3b*$^{Z\text{-}dta/+}$ animals have similar photoentrainment to controls with minor deficits in period lengthening. d, Percent activity in the dark portion of the ultradian cycle shows no significant difference between the genotypes. e, Quantification of phase shifts shows no significant differences between the two groups. f, Quantification of circadian period from the two groups under constant dark and constant light conditions. Both groups of animals show significant period lengthening under constant light. g) Venn diagram showing Brn3b-positive ipRGCs in yellow and Brn3b negative ipRGCs in green (full description is provided in supplementary table 1). ** indicates $p<0.01$, * indicates $p<0.05$ using student’s t-test. Error bars represent SEMs.